

## Ambient pressure and single-bubble sonoluminescence

Ljubinko Kondic\*

*Department of Mathematics and Department of Physics, Duke University, Durham, North Carolina 27708*

Chi Yuan

*Department of Physics, City College of the City University of New York, New York City, New York 10031*

C. K. Chan

*Institute of Physics, Academia Sinica, Nankang, Taipei, Taiwan, Republic of China*

(Received 16 September 1997)

We present a theoretical analysis of the influence of ambient pressure on single-bubble sonoluminescence (SBSL). By combining simulations of gas dynamics, mass diffusion theory, and stability analysis we find a narrow region of the parameter space where stable SBSL is possible. In particular, the theory predicts a 200% increase in SL radiation if ambient pressure is decreased only 5%. The results are compared with preliminary experimental data, and a good agreement is found. Variation of ambient pressure provides a simple and interesting test for the validity of various SL theories, diffusive or nondiffusive mass flow ideas, and stability analyses. [S1063-651X(98)51001-X]

PACS number(s): 78.60.Mq, 47.40.-x, 42.65.Re, 43.25.+y

Single-bubble sonoluminescence (SBSL) has been recently carefully explored, both experimentally (see [1] for a recent review) and theoretically. It has been determined that the light emitted from an oscillating gas bubble in liquids is of very short duration (less than 50 ps [2], or about 60–250 ps [3]), high emitted power (more than 30 mW), and that the spectrum of the emitted radiation shows similarities to the black body spectrum [4].

While there has been a variety of approaches to SBSL, the explanation based on the production of shock waves in an oscillating gas bubble seems most successful. Basic features of the SL radiation have been explained, including the extremely short time scale, high energy concentration [5–7], and the main characteristics of the radiated spectrum [6,7]. One of the interesting questions is the mass flow between the bubble and the surrounding liquid. Standard theory of rectified diffusion [8] seems not to be able to explain the existence of light-emitting air bubbles, which are stable with the respect to dissolution or growth during long periods of time [1,9]. Recently proposed theory resolves this problem by suggesting that chemical processes in an air bubble are responsible for the production of purely argon bubbles [10,11].

An additional insight to the problem of the mass flow and light emission mechanism could be reached by understanding the role of ambient pressure  $P_0$  in determining the equilibrium bubble size  $R_0$ , bubble dynamics in acoustic field, and SL radiation. Using diffusion theory [8,10–13] we calculate  $R_0$ ; its measurement will give a clear and simple answer to the question about the validity of the theory of rectified diffusion and “chemical” hypothesis mentioned above. With  $R_0$  given, SL radiation follows as a result of fully self-consistent computations of the dynamics of the gas in a bubble, coupled with radiative transport theory [7]. The question of the stability of a bubble with respect to non-

spherical perturbations is addressed as well [14–16]. Finally, as a result of this work, we are able to define the region of parameter space where stable SL is possible in experiments where  $P_0$  is varied. It is shown that  $P_0$  influences the character of SL radiation in a nontrivial manner, both through bubble dynamics and through  $R_0$ . We concentrate on the case of an air bubble in water, do not include the effects of gravity, and assume that the bubble remains spherical (except in the analysis of nonspherical perturbations); furthermore, thermal effects are included in a simple fashion through polytropic exponent [17]. All calculations are performed with standard values of air and water parameters at 20 °C.

The dynamics of the bubble follow from the Rayleigh-Plesset (RP) equation, modified in order to include the first order corrections proportional to  $\dot{R}/c_l$  (where  $\dot{R}$  is the velocity of the bubble-liquid interface, and  $c_l$  is the speed of sound in the liquid) [18]

$$R\ddot{R}\left(1 - \frac{\dot{R}}{c_l}\right) + \frac{3}{2}\dot{R}^2\left(1 - \frac{\dot{R}}{3c_l}\right) = \frac{1}{\rho_l}\left(1 + \frac{\dot{R}}{c_l}\right)\left[P_l(R,t) - P_0 - P_a\left(t + \frac{R}{c_l}\right)\right] + \frac{R}{\rho_l c_l} \frac{dP_l(R,t)}{dt}. \quad (1)$$

Here  $P_l(R,t)$  is the pressure in the liquid just next to the bubble wall, and  $P_a(t+R/c_l)$  is the time-delayed driving pressure. Ambient pressure is  $P_0$ , and liquid density is  $\rho_l$ . The relation between pressure in the gas  $P_g$ , and in the liquid,  $P_l = P_g - 2\sigma/R - 4\nu_l\rho_l\dot{R}/R$  closes the problem, assuming that  $P_g$  is known. For the purpose of calculating mass flow between the bubble and the liquid, and the stability of the bubble with respect to surface instabilities, we use  $P_g(V - V^{exc})^\kappa = \text{const}$ , where  $V$  is the volume of the bubble,  $V^{exc}$  is the excluded volume [7], and  $\kappa$  is the polytropic

\*Electronic address: Kondic@math.duke.edu

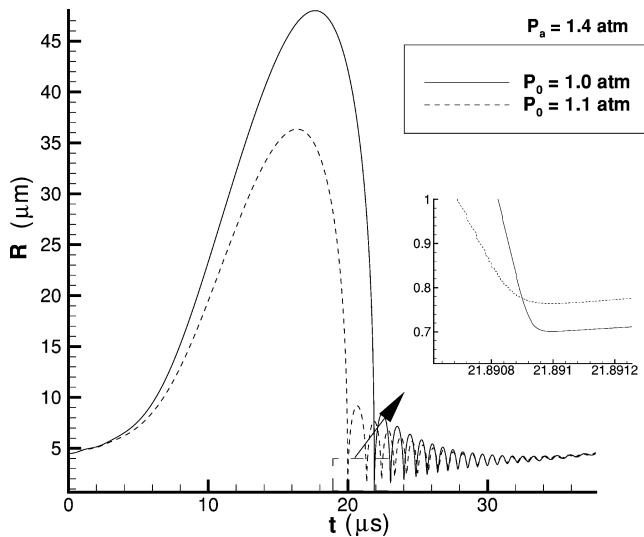


FIG. 1. Bubble radius versus time during one period of acoustic field, for two slightly different values of  $P_0$ . In the inset only first minima of the bubble radius are shown (the curve  $P_0=1.1$  atm is shifted). Note the decrease of the bubble velocity close to the minimum radius when  $P_0$  is increased.

exponent, which (crudely) includes the effects of heat flow between the bubble and the surrounding liquid [17].

In our simulations of the interior of the bubble, we relax the constraint of spatial uniformity of the gas, solve the gas dynamics equations, and obtain the required pressure in the gas next to the bubble wall [7]. We find a shock wave solution which breaks down the approximation of spatial uniformity of the gas; still, the results of our simulations show that the values of the pressure in the gas *next* to the interface are comparable to the values obtained from the polytropic model. In other words, we do not expect a strong influence of the shock propagation in the bubble on the dynamics of the bubble itself.

Let us now concentrate on two quantities that are of interest to us:  $P_0$  and  $R_0$ . Figure 1 shows that increase of  $P_0$  decreases the expansion ratio; in the inset of Fig. 1 we see that the velocity of the collapsing bubble is smaller as well. So, one expects weaker SL radiation. However, in what follows, it is shown that the variation of  $P_0$  also influences  $R_0$ , so the influence of  $P_0$  on the bubble dynamics and SL radiation is more involved.

$R_0$  follows from the dynamical condition that the mass outflow and mass inflow during an acoustic cycle are balanced. We account for diffusion of the gas from the bubble to the liquid, and also for rectified diffusion, which effectively leads to the flow of gas in the opposite direction [8,12,13]. The important parameter, which determines  $R_0$ , is the ratio of the concentration of the dissolved gas in the liquid  $c_i$ , and the saturation concentration  $c_0$ . Thus, we obtain the equilibrium bubble size that depends on applied acoustic pressure, normalized concentration of the gas, and ambient pressure.

In Fig. 2 each line gives the equilibrium values of  $R_0$ , for which total mass flow during one acoustic period is zero. In Fig. 2(a) the equilibrium is mostly unstable, since the slope of the curves is negative (our results for  $P_a=1$  atm differ slightly from [13], since we use a different bubble equation).

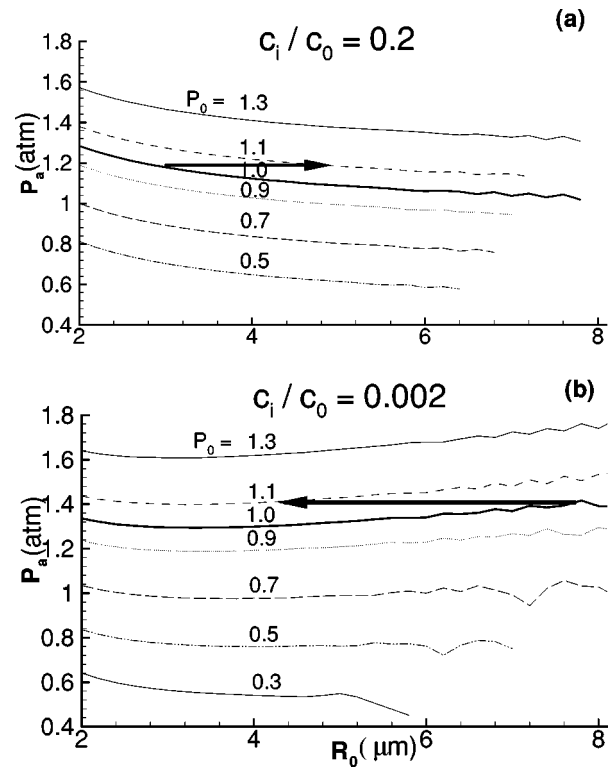


FIG. 2. Equilibrium bubble radius for a 20% air saturated water: (a)  $c_i/c_0=0.2$  (air is in the bubble); (b) relevant  $c_i/c_0=0.002$  (e.g., only Ar is left in the bubble). Dissolution (growth) occurs below (above) the curves. In (a) the equilibrium is mostly unstable. The lines with arrows show possible paths of  $R_0$  as  $P_0$  is increased from 1.0 to 1.1 atm.

The ratio  $c_i/c_0$  refers to its value for  $P_0=1.0$  atm, and is being modified if  $P_0$  is varied, in accordance with Henry's law. We choose  $c_i/c_0=0.2$ , since this is a commonly used experimental value. For larger values of  $R_0$  ( $>7$   $\mu\text{m}$  for  $P_0=1$  atm), period doubling and chaotic bubble oscillations are observed (not presented in Fig. 2). The lowest value of  $R_0$  for which period doubling occurs decreases as  $P_0$  is decreased.

Figure 2(a) shows that if  $P_0$  is increased, and  $P_a$  is kept constant,  $R_0$  has to jump to another curve, leading to an increase of  $R_0$  [a possible path is shown in Fig. 2(a)]. This is the observation that can be checked experimentally. On the other hand, this equilibrium is unstable; dissolution or growth could occur. However, the estimate of the time scale on which instability grows gives very long times measured in seconds [19].

We see that the diffusion theory alone is not able to explain *stable* mass equilibrium, which has been obtained in SL experiments with an air bubble. In what follows, we elaborate about the suggestion that there is some additional mass flow mechanism. In particular, we explore the recently suggested theory that chemical reactions inside an air bubble lead to the production of solvable products which leave the bubble, producing (almost) pure argon bubbles [10,11] (experimental support for this thesis appeared recently [9]). If this is the case, then the diagram where relevant concentration of the gas  $c_i/c_0 \approx 0.002$  is valid. This diagram is shown in Fig. 2(b).

Let us first concentrate on the curve corresponding to

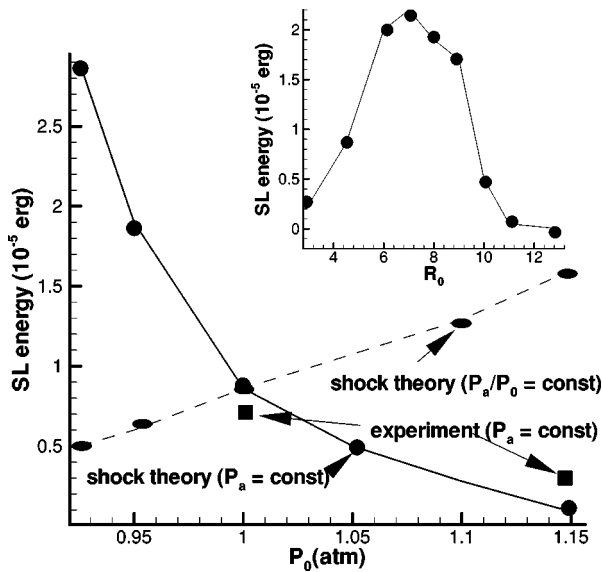


FIG. 3. SL radiation in the visible part of the spectrum. The circles (solid line) refer to fixed  $P_a = 1.4$  atm; the ellipses (broken line) to fixed ratio  $P_a/P_0 = 1.4$ . Experimental data are preliminary [20,21] and were obtained with 50% degassed water. The inset shows the dependence of SL intensity on  $R_0$ ; here  $P_0 = 1.0$  atm,  $P_a = 1.4$  atm.

$P_a = 1.0$  atm in Fig. 2(b). The equilibrium is now mostly stable, since the slope of the equilibrium curve is positive, at least for typical values of  $R_0$  used in experiments. In contrast to Fig. 2(a), the increase of  $P_0$  now leads to a decrease of  $R_0$  [a possible path is shown in Fig. 2(b)]. So, a variation of  $P_0$  and measurement of  $R_0$  can test the validity of the diffusion theory. One needs to determine whether  $R_0$  increases or decreases with an increase of  $P_0$ , and to determine whether the bubble is in the stable regime or not. As  $P_0$  is decreased, the slope of the equilibrium curves is decreasing, so that for  $P_0 \approx 0.3$  atm, it is mostly negative, meaning that it might not be possible to achieve stable equilibrium for small values of  $P_0$ . The experimental results are insufficient at this point. While some experiments have explored the variation of  $P_0$ , no results for  $R_0$  were given [1]. Our preliminary experimental results are not conclusive at this point [20,21]. However, it is interesting to note that SL has been obtained in water which was not degassed in the usual sense. An increase of  $P_0$  increases  $c_0$  (according to Henry's law), so the ratio  $c_i/c_0$  is effectively decreased, allowing for the existence of stable bubbles. We have observed stable sonoluminescence from nondegassed water with  $P_0 \approx 1.4$  atm [20,21].

What happens with SL radiation when  $P_0$  is varied? As mentioned earlier, an increase of  $P_0$  leads to weaker bubble oscillations, so less SL radiation is emitted. The other effect is the change of  $R_0$ , which also influences the intensity of SL radiation, at least if one assumes that SL radiation is emitted as the result of shock wave implosion. Figure 3 shows the results for the intensity of SL radiation following from the calculations of the gas dynamics [7]. There is a sharp decrease of SL intensity if  $P_0$  is increased and  $P_a$  kept constant, in agreement with preliminary experiments [20,21]. It is perhaps even more interesting that a decrease of  $P_0$  below 1 atm leads to strong increase of SL pulse (this effect has been recently experimentally observed [22]). If the ratio

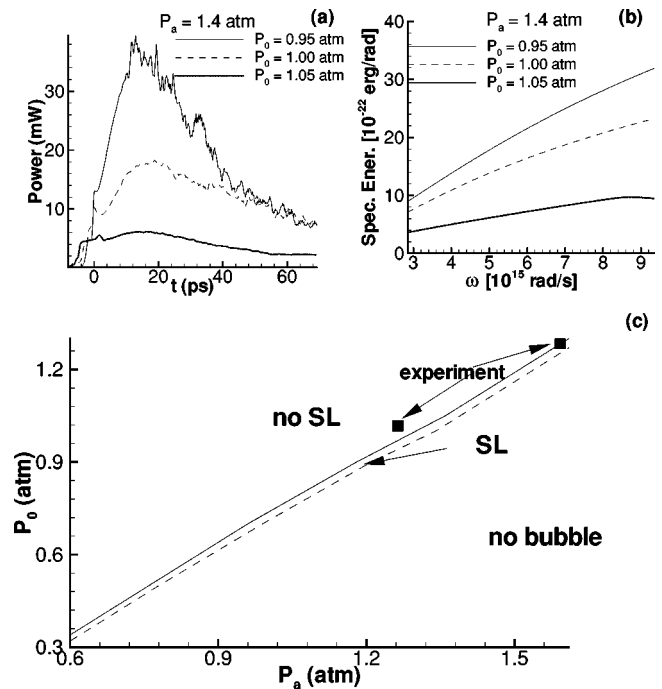


FIG. 4. (a) SL power.  $t=0$  is the time when the bubble velocity changes sign. (b) Spectrum of emitted SL pulse. (c) Phase diagram: SL is possible just in the small window between the threshold value of  $P_a$  for SL emission (solid line) and the onset of SI (broken line). The experimental values were obtained with 50% degassed water;  $R_0$  required for theoretical results was calculated using the “reduced” ratio  $c_i/c_0 = 0.005$ .

$P_a/P_0$  is kept constant, the change of SL radiation is weaker; in this case our calculations predict an increase of the intensity of SL radiation with an increase of  $P_0$ , due to the increase of  $R_0$  (the details depend also on  $c_i/c_0$ ).  $R_0$  is calculated assuming the “reduced”  $c_i/c_0 = 0.005$ , following the same approach which led to Fig. 2(b). The influence which  $R_0$  has on SL radiation is shown in the inset of Fig. 3. There is a value of  $R_0$  for which SL radiation is strongest; since  $R_0$  is defined by  $(P_a, P_0, c_i/c_0)$ , we understand why, e.g., a change in the degree of degassing leads to a change in the brightness of SL pulse.

Figure 4(a) shows the emitted power (in the visible part of the spectrum) versus time. It is important to note that the theory predicts that the duration of the SL pulse stays approximately constant when  $P_0$  is decreased, so the increase of SL radiation comes from the increase in the power of the pulse, not from the increased time of emission. In Fig. 4(b) we show the spectrum of emitted radiation. The spectrum is steeper for lower  $P_0$ ; this is another prediction that can be tested experimentally. When  $P_0$  is increased, the spectrum saturates for higher frequencies. We comment that the theoretical results given in Figs. 4(a) and 4(b) are in good qualitative agreement with experiments performed at  $P_0 = 1$  atm (e.g., [1]); calculated SL energy is slightly larger than the experimental one (theoretical results are not corrected for absorption of radiation in the water and in the flask walls), and the duration of the pulse (approximately 40 ps) is consistent with [1], but shorter than the recent results [3].

Finally, let us briefly address the question of bubble stability with respect to surface instabilities (SI). Here we con-

sider only parametric (Faraday) instabilities, and follow the approach developed by other researches in the field [14–16]; in particular, the viscous effects are assumed to be important only in a narrow boundary layer around the bubble [16]. Following the time evolution of a small azimuthal disturbance from the spherical shape, we calculate the Floquet transition matrix; the maximal eigenvalue serves as the criterion for instability (for details, see [16]). As the result, we obtain the SI line, which divides parameter space ( $P_a$ ,  $P_0$ ) into stable and unstable parts.

To the right of the SI (broken) line in Fig. 4(c), the bubble becomes unstable and eventually disappears. This typically happens for large values of  $P_a$ . The maximum “allowed” value of  $P_a$  increases as  $P_0$  is increased. This is expected, since increasing  $P_0$  reduces the intensity of bubble oscillations. For lower values of  $P_a$  [no SL regime in Fig. 4(c)], the shock theory predicts no SL radiation, since the oscillations are too weak to produce the imploding shock wave [7]. In the small region in between [SL in Fig. 4(c)], all conditions for SL radiation are satisfied.

Available experimental results for the onset of SI at  $P_0 = 1.0$  atm find the narrow region of allowed values of  $P_a$  about  $P_a = 1.20$  atm [9], so they are at slightly lower values than our theoretical results. Also, while the theory does predict that the size of the allowed range of  $P_a$  increases as  $c_i/c_0$  decreases, the theoretical range underpredicts the experimental one [1,9]. The polytropic approach might be one of the important factors leading to these discrepancies. Also, the results are very sensitive to the choice of gas and liquid parameters, e.g., if the viscosity of the liquid were doubled, the parametric instability line would have shifted to the right for about 0.1 atm, while the SL threshold would have not been modified significantly. This is probably the reason for

higher allowed values of  $P_a$  in the experiments performed at lower temperatures, where the viscosity of the water is higher [1]. Though the size and the position of the allowed region depend on the choice of parameters, the general trend of the results shown in Fig. 4(c) does not; the theory predicts approximately constant range of the allowed values of  $P_a$  as  $P_0$  is varied.

We present the analysis of the influence of ambient pressure on SBSL. It is shown that variation of ambient pressure influences SL emission through changes of bubble dynamics, and also through changes of equilibrium bubble size. SL radiation, calculated using previously developed simulations of gas dynamics, combined with radiative transfer theory, strongly increases with decrease of ambient pressure. The intriguing theoretical result is that both the minimum value of  $P_a$  that produces SL, and the lower threshold of  $P_a$  for SI increase approximately linearly with an increase of  $P_0$ . An increase of ambient pressure while the ratio  $P_a/P_0$  is kept constant leads also to (slow) increase of SL radiation. Further, mass diffusion theory allows one to calculate the equilibrium bubble radius as a function of ambient and acoustic pressures, and the degree of degassing. Assuming that only argon is left in the bubble, the theory predicts a decrease of equilibrium bubble size with an increase of ambient pressure. In particular, stable mass equilibrium might not be possible for small values of ambient pressure, less than 0.3 atm. Experimental verification of these predictions should bring us a step closer towards understanding of single-bubble sonoluminescence.

We thank Tom Chou and Detlef Lohse for useful discussions. This work was supported in part by DOE Grant No. DE-FG02-88ER25053 (L.K.).

- 
- [1] B.P. Barber, R.A. Hiller, F. Löfstedt, S.J. Putterman, and K.R. Weninger, *Phys. Rep.* **281**, 65 (1997).
  - [2] B.P. Barber and S.J. Putterman, *Nature (London)* **352**, 318 (1991).
  - [3] B. Gompf *et al.*, *Phys. Rev. Lett.* **79**, 1405 (1997).
  - [4] R. Hiller, S.J. Putterman, and B.P. Barber, *Phys. Rev. Lett.* **69**, 1182 (1992).
  - [5] C.C. Wu and P.H. Roberts, *Phys. Rev. Lett.* **70**, 3424 (1992); *Proc. R. Soc. London, Ser. A* **445**, 323 (1994).
  - [6] W.C. Moss, D.B. Clark, J.W. White, and D.A. Young, *Phys. Fluids* **6**, 2979 (1994); W.C. Moss, D.B. Clark, and D.A. Young, *Science* **276**, 1398 (1997).
  - [7] L. Kondic, J.I. Gersten, and C. Yuan, *Phys. Rev. E* **52**, 4976 (1995).
  - [8] A. Eller and H.G. Flynn, *J. Acoust. Soc. Am.* **37**, 493 (1964).
  - [9] R.G. Holt and D.F. Gaitan, *Phys. Rev. Lett.* **77**, 3791 (1996); *J. Acoust. Soc. Am.* **101**, 3060 (1997).
  - [10] D. Lohse *et al.*, *Phys. Rev. Lett.* **78**, 1359 (1997).
  - [11] S. Hilgenfeld and D. Lohse, *J. Chem Phys.* (to be published).
  - [12] L.A. Crum, *Ultrasonics* **1984**, 215.
  - [13] M.P. Brenner, D. Lohse, D. Oxtoby, and T.F. Dupont, *Phys. Rev. Lett.* **76**, 1158 (1995).
  - [14] A.I. Eller and L.A. Crum, *J. Acoust. Soc. Am.* **47**, 762 (1970).
  - [15] A. Prosperetti, *Q. Appl. Math.* **34**, 339 (1977).
  - [16] M.P. Brenner, D. Lohse, and T.F. Dupont, *Phys. Rev. Lett.* **75**, 954 (1995); S. Hilgenfeldt, D. Lohse, and M.P. Brenner, *Phys. Fluids A* **8**, 2808 (1996).
  - [17] A. Prosperetti, *J. Acoust. Soc. Am.* **61**, 17 (1977).
  - [18] A. Prosperetti and A. Lezzi, *J. Fluid Mech.* **168**, 457 (1986).
  - [19] D.F. Gaitan, L.A. Crum, C.C. Chuch, and R.A. Roy, *J. Acoust. Soc. Am.* **91**, 3166 (1992).
  - [20] L. Kondic, C.K. Chan, and C. Yuan, *J. Acoust. Soc. Am.* **100**, 2678 (1996).
  - [21] C.K. Chan, C. Yuan, and L. Kondic (unpublished).
  - [22] T. Matula (private communication).